Open Research Europe

Connecting Complex and Simplified Models of Tipping Elements: A Nonlinear Two-Forcing Emulator for the Atlantic Meridional Overturning Circulation

Amaury Laridon[1], Victor Couplet[2], Justin Gérard[2], Wim Thiery[1], Michel Crucifix[2]

[1]Vrije Universiteit Brussel, Department of Water and Climate, bclimate Research Group, Brussels, Belgium.
[2]UCLouvain, Earth and Life Institute, Louvain-La-Neuve, Belgium.
Corresponding author : Amaury.Laridon@vub.be

Abstract

Despite the likely future collapse of the Atlantic Meridional Overturning Circulation (AMOC) and its profound potential impacts, accurately assessing its tipping dynamics remains a major challenge. Complex models, such as Earth System Models (ESMs) and Earth System Models of Intermediate Complexity (EMICs), exhibit significant uncertainties in pinpointing the AMOC's tipping point and collapse dynamics. Recent research has focused on developing conceptual models based on non-linear dynamics to capture the behaviour of such tipping elements. However, existing conceptual emulators typically simulate the AMOC's response to a single temperature forcing, despite the well-established influence of freshwater flux on its dynamics. Furthermore, current two-forcing conceptual models lack a robust calibration method based on complex models. In this study, we develop and validate a novel AMOC emulator incorporating two forcing parameters—global mean temperature and freshwater flux—based on non-linear dynamics. This emulator is applied to simulate the AMOC response within cGenie, an EMIC. Upon validation, the emulator is integrated into SURFER, a reduced-complexity climate model, enabling rapid and efficient simulations of AMOC trajectories across various emission scenarios. By facilitating a larger number of simulations than complex models while maintaining calibration accuracy, this tool represents a significant advancement in exploring the future behaviour of the AMOC. Additionally, the methodology used to develop this two-parameter emulator is highly generalizable and can be applied to other tipping elements, offering valuable insights for future studies on tipping element dynamics.

Plain Language Summary

As global temperatures rise due to greenhouse gas emissions, some key components of the Earth's climate system are approaching critical thresholds, beyond which major changes may occur. One such component is the Atlantic Meridional Overturning Circulation (AMOC), a crucial ocean current responsible for redistributing heat between the Southern and Northern Hemispheres. If the AMOC were to collapse, it could lead to significant regional changes in temperature, precipitation patterns, and other critical aspects of the climate. However, the exact location of the AMOC tipping point and the time it would take to collapse remain uncertain due to limitations in complex climate models. Additionally, running these complex models is computationally expensive, making it difficult to explore a wide range of potential future scenarios. In this study, we developed an emulator—a simplified conceptual model calibrated using a complex model—to reproduce the key behaviours of the AMOC during a potential collapse. This emulator is based on a novel methodology that allows for more accurate alignment between simplified dynamics and complex models. The resulting tool enables large-scale simulations of AMOC behaviour under various emission scenarios with low computational cost while maintaining consistency with our understanding of the physical processes governing the AMOC. By improving the efficiency of fast climate simulations, this approach helps researchers better investigate the potential responses of the AMOC to future emission scenarios and enhances our ability to predict and prepare for critical changes in the climate system.

Keywords

Climate change, Tipping Points, AMOC, Emulator, Non-linear dynamics, SURFER, cGenie.

1. Introduction

1.1 The AMOC as a Tipping Element: Addressing High Uncertainties

The Atlantic Meridional Overturning Circulation (AMOC) is a critical component of the climate system, playing a central role in the transport of heat and salt throughout the global ocean and significantly influencing both regional and global climate dynamics (1–3). The AMOC has been identified as a tipping element, a large-scale component of the climate system that can reach a tipping point (4). A tipping point refers to a critical threshold in a forcing parameter, known as the bifurcation parameter, beyond which a small perturbation of this parameter can cause the tipping element to transition from one equilibrium state to another, resulting in a significant qualitative change (4). For the AMOC, the secondary stable equilibrium corresponds to a collapse state, where the circulation ceases (5). A cessation or even a slowdown of the AMOC would have significant consequences for temperatures in the North Atlantic (3–6), as well as impacts on the carbon cycle (7), monsoons (2), and, crucially, other tipping elements (5,8,9).

Effectively simulating the AMOC requires an understanding of its physical dynamics. The AMOC operates through the sinking of large amounts of warm, salty water from the South Atlantic into the North Atlantic. As this water cools, it becomes sufficiently dense to sink into the depths, forming the North Atlantic Deep Water (NADW), which then returns to the South Atlantic (10,11). The AMOC is also referred to as the thermohaline circulation because it is driven by density differences, which are determined by the temperature and salinity of the water. The tipping point of the AMOC corresponds to a critical threshold in the stratification of Atlantic waters. With global warming, the increase in Atlantic water temperature reduces its density, thereby enhancing its buoyancy (12). This thermal forcing is the dominant mechanism driving AMOC weakening (13,14). The second forcing mechanism involves a disturbance in the salinity of the water within the Atlantic. As the Greenland Ice Sheet (GIS) melts due to global warming, large quantities of freshwater are added to the deep-water sinking regions in the North Atlantic. This freshwater flux reduces the water's density, increasing its buoyancy and diminishing its ability to sink into the depths, thereby weakening the intensity of the AMOC (15–17). Therefore, regardless of the combination of these two forcing mechanisms—which together form the bifurcation parameter of the AMOC—there exists a critical threshold of water stratification that, if exceeded for a prolonged period (18), can become self-sustaining because the AMOC can no longer bring warm and salty water to the North of the Atlantic (19) and hence ultimately lead to the collapse of the circulation (5,15,20). Once reached, this collapse state is irreversible, as returning to the critical value of the bifurcation parameter will not allow the system to return to its initial equilibrium. A characteristic hysteresis phenomenon is thus present, preventing a return to the initial state within timescales relevant to human lifetimes (4,21).

There is evidence that the AMOC has slowed during the 20th century (22), with inferred reconstructions indicating a 15% decline over the past 70 years (23), bringing it closer to its tipping point. However, observations of AMOC slowdown are subject to considerable uncertainty (10), and although the AMOC may have collapsed in the past (8,24,25), accurately forecasting its future evolution—when and at what rate it may collapse remains a significant challenge (5,26,27). Estimates of the tipping point for the AMOC must therefore rely on models, but the results vary significantly (27). Some studies place it at a global mean temperature anomaly of 8°C, while others suggest it may already be as low as 8°C (28). Consequently, some studies estimate that a complete collapse of the AMOC could occur by the end of this century (29), or not until 2300 (15).

1.2 The Need for Simplified Models Capturing First-Order Dynamics

This significant uncertainty regarding the future evolution of AMOC collapse stems from the diversity of models employed. While complex models such as Earth System Models (ESM) might theoretically be the most suitable tools for studying the AMOC, they are incapable of simulating complete AMOC hysteresis curves due to their prohibitive computational demands (30). Consequently, the models best equipped to compute quasi-equilibrium thermohaline hysteresis curves are Earth System Models of Intermediate Complexity (EMIC) (26,31). However, EMICs show significant variability in the location of

the tipping point and, thus, in their projections of the AMOC future evolution (26). Moreover, due to their substantial computational costs, these models are not well-suited for efficiently exploring the space of potential forcing scenarios and their associated AMOC responses. Therefore, recent approaches in the literature have focused on using conceptual models to simulate the AMOC and other tipping elements (32–35).

This approach primarily relies on modelling the dynamics of tipping elements through a double-fold bifurcation structure (32,33,35), as stability indicators and observational analyses have shown that the AMOC resides in a bi-stable regime (36–38). In this framework, the system possesses two stable equilibria separated by an unstable equilibrium. When the bifurcation parameter reaches the critical value of the tipping point, the system can transition from its initial stable equilibrium to the second. These models mathematically impose that the AMOC behaves as a nonlinear dynamical system with this specific double-fold structure, thereby defining its intrinsic tipping element dynamics.

The primary advantage of these models, beyond their ability to capture the suspected dynamical behaviour, is their computational efficiency. By calibrating these simplified dynamics using experiments from complex models, these models enable the creation of tipping element emulators. When these tipping element emulators are coupled with a reduced-complexity climate model, they offer a tool that is both process-based and computationally efficient. This enables the study of tipping element evolution in multi-millennial simulations under realistic emissions scenarios (32).

1.3 Challenges in Designing a Two-Forcing Emulator

An emulator based on the concept of a double-fold bifurcation was introduced by Martinez Montero et al.(39) in the reduced-complexity climate model SURFER v2.0 to simulate the dynamics of ice sheets. However, this emulator considered only a single forcing variable, specifically the temperature anomaly. Introducing an additional forcing variable necessitates the inclusion of a corresponding parameter that must be calibrated, a task that is both challenging and non-trivial. In SURFER v3.0, Couplet et al. (32,40) developed a generalization of this emulator, allowing for the coupling of tipping elements and hence the inclusion of an additional forcing variable. The challenge, however, lies in establishing a calibration technique for the model parameters based on existing literature and complex models. In their study, Couplet et al. (32) employed a Monte Carlo sampling method within the parameter space of their simplified models to reproduce the configurations considered plausible in the literature regarding the state of tipping elements. Nevertheless, as highlighted in their study (32), developing an emulator with a two-forcing model of tipping elements that can be calibrated to any specific hysteresis curve from a complex model is both valuable and necessary. Such an approach would enable more realistic calibration of the conceptual model's parameters. Furthermore, it would facilitate the exploration of the forcing space across different emissions scenarios over long timescales, while preserving the characteristics of the emulated EMICs. This would result in realistic yet computationally inexpensive simulations.

To date, no simplified tipping element model with two forcing parameters, capable of being calibrated using experiments from complex models, has been developed. However, the AMOC is influenced by two forcing variables: temperature anomaly and freshwater flux. Given the necessity of more realistically constraining potential future AMOC trajectories, this study seeks to address the following scientific question: How can we develop an AMOC emulator with two forcing parameters − temperature and freshwater flux − that can be calibrated against hysteresis from complex models and integrated into a climate model? The paper is structured as follows. In Section 2, we introduce the AMOC Tipping Calibration Model (ATCM), a simplified nonlinear dynamical model based on the double-fold bifurcation structure with two forcing parameters: temperature anomaly and freshwater flux. We also describe the calibration module used to fit the double-fold structure to any hysteresis curve derived from a complex model. This novel module is based on the assumption of independent forcing calibration experiments, which allows for a generalization of the method by Martinez Monteiro et al. (39), though it also introduces approximations. In Section 3, we apply this calibration process to cGenie, an Earth System Model of Intermediate Complexity (EMIC), using two calibration experiments. We then validate the

Commented [AL1]: Not sure of the relevance of this. Does this need to be highlight the challenge of the task ?

Commented [AL2]: Is it needed to already say that at that point ?

ATCM as an emulator by comparing its results with those of one additional cGenie experiment. Subsequently, we integrate the ATCM into the SURFER climate model, creating a new configuration that provides a calibrated emulator of the AMOC within a fast climate model. This setup enables the analysis of overshoot without tipping phenomena, as well as the impact of coupling between the AMOC and the Greenland Ice Sheet (GIS). Furthermore, it paves the way for additional investigations into the potential collapse dynamics of the AMOC under realistic emission scenarios. Section 4 analyses our key findings, comparing them with previous studies. It also discusses the limitations of our approach in emulating a complex dynamic using a conceptual non-linear dynamics model and outlines perspectives for improving this methodology and applying it to emulate other tipping elements. Finally, we conclude in Section 5.

Commented [AL3]: To be update if we add this part or not

2. Methods

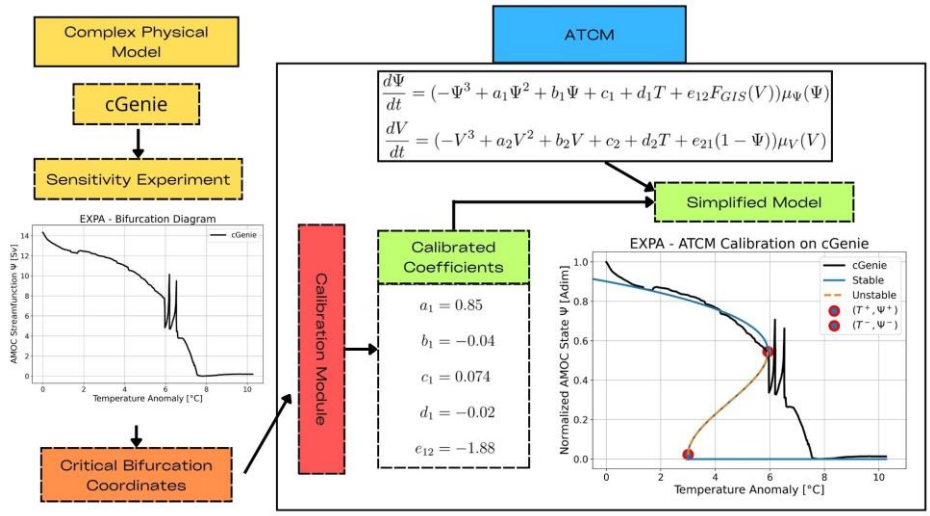

Figure 1 : Schematic of the AMOC Tipping Calibration Module (ATCM). The module requires input in the form of critical bifurcation coordinates derived from complex experiments. These coordinates are used to adjust the calibration coefficients within the simplified tipping element model.

In this methods section, we introduce the AMOC Tipping Calibration Module (ATCM), an emulator designed to represent the dynamics of the AMOC tipping element, based on a double fold non-linear dynamical system with two forcing parameters: temperature and freshwater flux. The key feature of this emulator is its ability to calibrate simplified AMOC dynamics to match any hysteresis curve derived from more complex, process-based models. We detail the equations that define the model and describe the methodology used for its calibration. The AMOC model is inspired by the work of Couplet et al. (32), while the calibration technique extends the ice sheet emulator implemented in SURFER v2.0 (39) by utilizing the assumption of independent forcing in the calibration experiments. Subsequently, in the results section, the ATCM is calibrated using the cGenie model, enabling it to act as an emulator for the AMOC. Once integrated into the SURFER reduced-complexity climate model, it allows for fast and calibrated simulations of potential future evolutions of the AMOC

Commented [AL4]: Is it need here in the introduction of the methods section ?

2.1 AMOC Dynamical Model

The overall scheme of the ATCM is depicted on Fig.(1). Given that the freshwater flux forcing in the ATCM is intended to represent the flux associated with the melting of the Greenland Ice Sheet (GIS), we also provide an explicit mathematical formulation of the GIS model, which will be used in the SURFER

reduced-complexity climate model. The non linear ordinary differential equations that describes the AMOC intensity and the GIS volume are written as,

$$\frac{d\Psi}{dt}(\Psi, T, F_{GIS}) = \left(\overbrace{-\Psi^3 + a_1\Psi^2 + b_1\Psi + c_1}^{\text{internal dynamics}} + \overbrace{d_1 T + e_{12} F_{GIS}}^{\text{forcings}} \right) \mu_\Psi(\Psi), \quad (1)$$

$$\frac{dV}{dt}(V, T, \Psi) = \left(\underbrace{-V^3 + a_2 V^2 + b_2 V + c_2}_{\text{internal dynamics}} + \underbrace{d_2 T + e_{21}(1-\Psi)}_{\text{focings}} \right) \mu_V(V). \quad (2)$$

These equations are derived from the normal form of a double-fold bifurcation, enabling the representation of the first-order tipping dynamics of the AMOC and the GIS. Consequently, the tipping element model acts as a generic dynamical system designed to function as an emulator. The use of a generalized normal form of a double-fold bifurcation has already been demonstrated to be effective for tipping element models (32,35,39). The state variable Ψ and V are dimensionless variables spanning the interval $[0, 1]$ that defines the state of the AMOC and the GIS respectively compare to their pre-industrial state. For the AMOC it is the ratio of its current intensity in Sv with its pre-industrial value while for the GIS is the ice volume compare to its pre-industrial value. The first group of terms in Eq.(1,2) represents the internal dynamics of the tipping element. Since it is a cubic polynomial of the state variable x, it allows or the tipping element to have 1,2 or 3 stable states depending on the values of its forcings (32). The various coefficients $a_i, b_i, c_i, d_i, e_{ij} (i, j = 1,2, i \neq j)$ do not correspond to specific physical processes but collectively allow the simplified model to be calibrated to the desired steady-state structure of the complex model being emulated. These are the parameters of the simplified model that will be calibrated using the calibration module described in this section.

Regarding the forcing terms in both Eq.(1) and Eq.(2), the first forcing term, T represents the global mean atmospheric temperature anomaly relative to pre-industrial levels. This term encapsulates the effects of warming on AMOC water stratification, leading to a weakening of its intensity, as well as the impact on ice melting for the GIS. In Eq.(1), the second forcing term, F_{GIS}, represents the freshwater flux resulting from GIS melting, which weakens the intensity of the AMOC. The parameterization of F_{GIS} is based on that of Couplet et al. (32) and is defined as follow,

$$F_{GIS} = \alpha_{GIS} \dot{V}. \quad (3)$$

The rate of melting of the GIS, and thus its freshwater contribution, is evidently proportional to the temporal variation of its volume $\dot{V} = \frac{dV}{dt}$. The parameter α_{GIS} relate the temporal variation of the dimensionless fraction of the GIS to a freshwater flux. The details of the computation and the value of α_{GIS} are provided in Couplet et al.(32). Through this parameterization of F_{GIS}, we establish a dynamic dependence of the AMOC on the state of the GIS that is useful to study tipping cascade interactions between the AMOC and the GIS as shown in Couplet et al.(32). Finally, it is known that a collapse of the AMOC, due to its regional cooling, will stabilize the melting of the GIS (5). In Eq.(2) the second forcing variable is the state of the AMOC. By using a parameterization $(1 - \Psi)$ this ensures that the stabilizing effect of the AMOC on the GIS is maximum when the AMOC has collapse $\Psi = 0$.

The functions $\mu_\Psi(\Psi)$ and $\mu_V(V)$ represent inverse time scales that describe the intrinsic dynamics of the tipping elements (32). Denoting either of the two state variables as x, these functions are defined as follows,

$$\mu_x(x) = \begin{cases} \frac{1}{\tau_x^+} & if \quad \frac{dx}{dt} > 0 \ \ and \ \ 0 < x < 1, \\ \frac{1}{\tau_x^-} & if \quad \frac{dx}{dt} < 0 \ \ and \ \ 0 < x < 1, \\ 0 & if \quad x \leq 0 \ \ or \ \ x \geq 1. \end{cases} \quad (4)$$

We define two distinct time scales for the dynamics of the tipping elements to represent the asymmetry

inherent in processes associated with the GIS, as ice melting typically occurs more rapidly than ice formation. τ_x^+ represents the characteristic timescale of the intrinsic dynamics of the element transitioning from its collapsed state to its nominal state, whereas τ_x^- represents the characteristic timescale for the reverse transition, from the nominal state to the collapsed state. The third case in Eq.(4) ensures that the normalized state of the tipping element, x, remains between the value $x = 0$ for the completely collapsed state and $x = 1$ indicating the initial pre-industrial state. The internal timescale dynamics are a critical parameter in the evolution of tipping elements, and accurately estimating these parameters remains a significant challenge (5,28). In the results section, we will calibrate the values of τ_Ψ^+ and τ_Ψ^- based on a tuning procedure to reproduce the internal timescale dynamics of the AMOC in cGenie. For the GIS, we set $\tau_V^+ = 5500$ years and $\tau_V^- = 700$ years, based on reasonable values derived from the literature review by Armstrong McKay et al.(28) and Couplet et al.(32). The objective is to develop and validate the ATCM as an emulator of the AMOC. Since the freshwater flux forcing will be parameterized to replicate that used in the cGenie simulations, the exact values of the $\tau_V^\pm$ parameters are not critical for this study; however, they are based on specific studies (28).

Commented [AL5]: To be update

2.2 Calibration Module

Now, we aim to develop a calibration algorithm that, based on the critical coordinates of bifurcation points obtained from hysteresis experiments of complex models, will calibrate the parameters $a_i, b_i, c_i, d_i, e_{ij} (i, j = 1,2, i \neq j)$. In this paper, we focus on validating the calibration methods for the AMOC. However, the translation to any simplified model based on the normal form of a bifurcation, such as Eqs. (1, 2), which include two forcings, can be performed easily. For instance, the translation for the GIS calibration is provided in the Appendix. For the calibration, we seek to find the best fit for our double-fold structure to the complex hysteresis, ensuring that our simplified dynamics pass through the bifurcation points identified in the process-based hysteresis. In the paper describing the SURFER v2.0 model, Martinez-Montero et al.(39) develop a mathematical framework that allows, in the case of the Antarctic and Greenland ice sheet - also modelled by a canonical double-fold normal form - to be calibrate from more complex experiments by the retrieval of the coordinates of the bifurcation points. From an epistemological standpoint, the significant advantage of the Martinez-Monteiro et al.(39) method is to provides semantics with both physical coherence and meaning to the calibration parameters. By defining these parameters in terms of the coordinates of the bifurcation points given by the complex model under study, we obtain the double-fold structure behinds the process-based experiments. This methods also allows to test the underlying hypothesis that the leading-order dynamics of tipping elements such as the AMOC can be captured by a double-fold. These are the reasons why we aim to adhere to the calibration framework proposed by Martinez-Monteiro et al.(39). However, the mathematical framework presented by Martinez-Monteiro et al.(39) for modelling each individual ice sheet relies on a single ordinary differential equation with only one forcing parameter, namely the temperature anomaly. In our case, for the AMOC, we have two forcing parameters: the temperature anomaly and the freshwater flux.

To develop a calibration technique for our double-fold dynamics of the AMOC with two forcing parameters, we will generalize the method of Martinez-Monteiro et al. (2022), based on an operational assumption. We make the assumption that the complex models we will use to calibrate the hysteresis of the AMOC allow for independent forcing of the AMOC. In other words, if we take our ATCM model for the AMOC (see Eq.(1)), we should be able to access process based models that can force the AMOC solely through temperature anomaly while keeping the freshwater flux forcing constant, and vice versa. Fortunately, due to the construction of the vast majority of climate models, this is technically entirely feasible If the aim is also to emulate the transition from the collapsed state to the nominal state, an additional constraint arises in the selection of complex models. Specifically, the complex models must be capable of conducting hysteresis experiments, which involve simulations where the tipping element remains in equilibrium and thus require large temporal scales. For instance, in the cGenie experiments used for calibration of collapse dynamics, simulations span over 20,000 years (see Appendix). This requirement implies that complex models categorized as EMICs are suitable targets for emulation, as these models can perform simulations over extensive timescales while maintaining physical consistency (30).

The recipe for our calibration, which is generalizable to N forcings, is as follows. To calibrate the coupling parameters associated with the N forcing variables, we perform N independent sensitivity experiments to independently calibrate the associated bifurcation diagrams by systematically reducing the calibration to a Martinez-Monteiro et al.(39)-type model with only one forcing variable, as the other $N-1$ variables become constants. For the AMOC, $EXPA$ is defined as the calibration experiment of the AMOC intensity with respect to a temperature forcing, conducted using any complex model that satisfies the aforementioned conditions. From this experiment we can retrieve the coordinates of the bifurcation points denoted by,

$$(\Psi^+, T^+), (\Psi^-, T^-). \tag{5}$$

In this context, $\Psi^{\pm}$ represents the normalized values of the AMOC intensity, where the system transitions from its nominal stable equilibrium state (Ψ^+) to its collapsed equilibrium state, and from the collapsed equilibrium state (Ψ^-) back to the nominal equilibrium state. The $T^{\pm}$ values denote the critical temperature anomaly forcing at which a bifurcation occurs within the system. The Eq.(1) in the $EXPA$ experiment can be written as,

$$\frac{d\Psi}{dt}\left(-\Psi^3 + a_1\Psi^2 + b_1\Psi + c_1 + d_1 T + e_{12}F_{GIS}^A\right)\mu_\Psi(\Psi), \tag{6}$$

where F_{GIS}^A represents the arbitrary constant value of the freshwater flux forcing applied during the simulation in the complex model. Consequently, $c_1 + e_{12}F_{GIS}^A$ is a constant term in this experiment, effectively reducing the conceptual model to a single-forcing experiment. This simplification enables the application of the calibration technique proposed by Martinez Montero et al.(39) to determine the parameters.

$$a_1 = \frac{3(\Psi^- + \Psi^+)}{2} \tag{7}$$

$$b_1 = -3\Psi^-\Psi^+ \tag{8}$$

$$c_1 = \frac{T_\Psi^+\Psi^{-^2}(\Psi^- - 3\Psi^+) - T_\Psi^-\Psi^{+^2}(\Psi^+ - 3\Psi^-)}{2(T_\Psi^- - T_\Psi^+)} - e_{12}F_{GIS}^A \tag{9}$$

$$d_1 = -\frac{(\Psi^+ - \Psi^-)^3}{2(T_\Psi^+ - T_\Psi^-)} \tag{10}$$

We define $EXPB$ as the second calibration experiment examining the AMOC intensity response to freshwater forcing, conducted using the same complex model. In this experiment, the freshwater flux parameterization in the complex model is designed as a hosing experiment to simulate the effects of GIS melting. From this experiment, we can extract the coordinates of the bifurcation points,

$$(\Psi^+, F_{GIS}^+), (\Psi^-, F_{GIS}^-). \tag{11}$$

F_{GIS} represents the critical values of the freshwater flux forcing at which the bifurcation of the AMOC occurs. By defining T_B as the constant value of the temperature anomaly imposed during the complex model experiment, Eq.(1) can be expressed as:

$$\frac{d\Psi}{dt}(-\Psi^3 + a_1\Psi^2 + b_1\Psi + c_1 + d_1 T^B + e_{12}F_{GIS})\mu_\Psi(\Psi). \tag{12}$$

Here, $c_1 + d_1 T^B$ represents the constant term, and the method proposed by Martinez Monteiro et al. (39) enables the determination of two new values for the following parameters,

$$c_1 = \frac{F_{GIS}^+\Psi^{-^2}(\Psi^- - 3\Psi^+) - F_{GIS}^-\Psi^{+^2}(\Psi^+ - 3\Psi^-)}{2(F_{GIS}^- - F_{GIS}^+)} - d_1 T^B, \tag{13}$$

$$e_{12} = -\frac{(\Psi^+ - \Psi^-)^3}{2(F_{GIS}^+ - F_{GIS}^-)}, \tag{14}$$

Thus, based on the five unknowns $(a_1, b_1, c_1, d_1, e_{12})$, the assumption of independent calibration experiments allows us to apply the methodological framework of Martinez Monteiro (39) to a single forcing variable. This results in six equations with an over-determination of the independent parameter c_1. The application of this method to calibrate the GIS model, Eq. (2), is provided in the Appendix. For the GIS case, it requires a complex model capable of simulating its volume projections with independent forcing possibilities for the AMOC and temperature.

With this methodological framework, it is also possible to generalize the approach to include more than two forcing parameters. For instance, as demonstrated in the Appendix, an additional freshwater flux forcing term was incorporated into Eq.(1) to calibrate the impact of variations in the evaporation-precipitation balance over the Atlantic basin under future scenarios. Mathematically, the generalization to N forcing variables results in obtaining $4N - 2(N-1)$ equations with $4 + (N-1)$ knowns, leading to $N-1$ over-determined equations. As will be shown in the next section with the emulation of cGenie, these over-determinations reflect the fact that the coefficient c_1 is the shared constant across all calibrations of different sensitivity experiments. It represents the component of the model that must adjust for each sensitivity experiment while remaining consistent across all of them. What value, then, should be assigned to c_1? Sensitivity experiments have demonstrated that defining $c_1 = c_1^A$, where c_1^A is determined from Eq. (9), yields the most accurate results. This is because temperature forcing is the primary driver of AMOC collapse, as demonstrated, for instance, in CMIP5 experiments (13). Consequently, we prioritize achieving the best calibration for temperature forcing, while accepting a greater margin of error in the calibration of freshwater flux forcing.

The final parameter in the ATCM module that needs to be calibrated is the typical internal dynamic time scale of the AMOC, denoted as $\tau_\Psi^{\pm}$. Based on Armstrong McKay et al.(28) we assume that the internal dynamic time scale of the AMOC from its nominal stable state to its collapse stable state is the same, i.e., $\tau \equiv \tau_\Psi^+ = \tau_{\overline{\Psi}}$. To calibrate this parameter, the proposed experimental setup involves running a simulation with the complex model to be emulated, using a stepwise parametrized forcing of the freshwater flux while maintaining a fixed temperature forcing. For instance, the simulation can start with a 0 Sv forcing, then incrementally add 0.05 Sv to slow down the AMOC, gradually decrease the forcing by 0.05 Sv until the value reaches -0.05 Sv, and repeat this procedure several times. The goal is to obtain a time series of the AMOC intensity with several instances where the AMOC is being reduced. Based on these experimental data, a manual tuning of τ within ATCM allows for determining the best value to replicate the characteristic time scale of AMOC dynamics in the complex model.

3. Results

In this results section, we first calibrate the ATCM using cGenie, an EMIC, through three calibration experiments labelled $EXPA$, $EXPB$, and $EXPC$. The first two experiments are used to calibrate the coefficients $a_1, b_1, c_1, d_1, e_{12}$, while $EXPC$ is employed to calibrate the parameter τ. Second, we validate the effectiveness of the ATCM by simulating an AMOC trajectory under a forcing configuration different from the calibration experiments and comparing the results with the original cGenie simulation. Finally, we integrate the ATCM into SURFER to demonstrate the emulator's capability to efficiently sample the forcing space under realistic emission scenarios.

Commented [AL6]: Add overshoot analysis if performed

3.1 Calibration with cGenie

To validate the emulator, we applied the ATCM to cGenie (41), an EMIC (31) that has already demonstrated its ability to simulate AMOC hysteresis (14,42). cGenie includes an ocean circulation model (3D), a dynamic-thermodynamic sea ice model (2D) and an atmospheric energy moisture balance model (2D). The ocean model accounts for the horizontal and vertical transport of heat, salinity and biogeochemical tracers. The circulation is simulated through advection, convection, and mixing. Following the experimental framework outlined in the Methods section, we conducted two independent sensitivity calibration experiments on the AMOC intensity using cGenie.

The first experiment, labelled $EXPA$, consisted of a 20,000 years simulation with a prescribed CO_2 forcing designed to generate a global atmospheric mean temperature anomaly. The forcing was parameterized as a linear function, increasing from 280 ppm to 2,800 ppm. Through the internal dynamics of cGenie, this forcing is translated into a global mean 2-meter surface air temperature anomaly, starting from $T = 0°C$ for the initial thousands of years and reaching $T = 10°C$ after 20,000 years (see Fig. S1). This setup enabled us to cover the plausible range of the AMOC tipping point location in terms of temperature forcing (5,28) while ensuring near-equilibrium conditions for the AMOC.

The second independent sensitivity calibration experiment, labelled $EXPB$, involved a 20,000 years hosing simulation with freshwater flux forcing ranging from 0 Sv to 0.2 Sv. These values were chosen to align with the plausible range of AMOC tipping point locations related to freshwater forcing (17,26) and to be sufficient to trigger an AMOC collapse in cGenie. The forcing was again parameterized using a linear function (see Fig. S2), and the freshwater hosing was applied between $50°N$ and $70°N$ and $45°W$ to $5°E$ (see Fig. S3) to simulate the regions of freshwater input from GIS melting. The durations of the $EXPA$ and $EXPB$ simulations were chosen to ensure that the AMOC is forced sufficiently slowly, allowing it to remain in equilibrium and produce the collapse branch of the hysteresis.

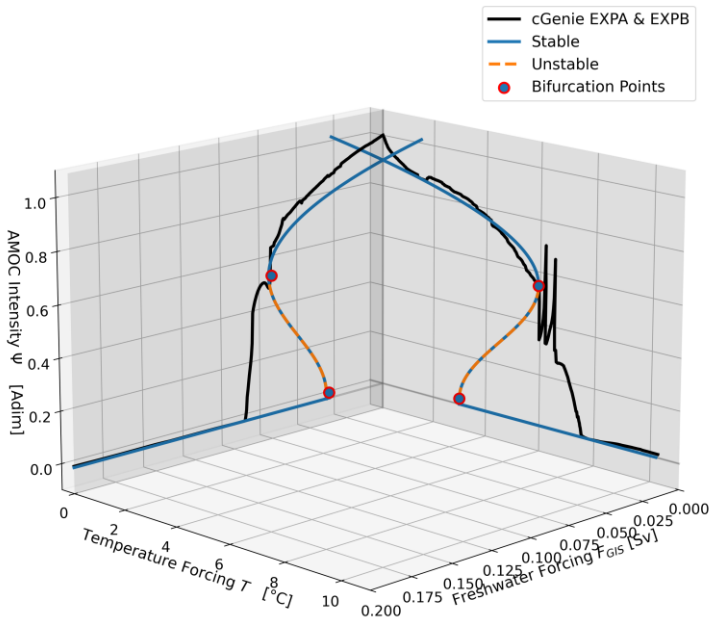

Figure 2 : Bifurcation diagrams of cGenie and ATCM in the (T, F_{GIS}) forcing space. The two hysteresis loops produced by cGenie during the calibration experiments $EXPA$ and $EXPB$ are shown in their respective planes as solid black lines. The identification of the bifurcation points based on these hysteresis loops is marked in red, while the simplified hysteresis produced by the ATCM is shown in blue. The trajectory of the unstable equilibrium, which separates the two stable equilibria, is represented by the orange dashed line.

The two hysteresis obtained with cGenie in the $EXPA$ and $EXPB$ experiments are shown in Fig.(2). Since the primary objective of the ATCM is to accurately calibrate the stable branch of the nominal state and its collapse, we focused exclusively on simulating collapse scenarios with the complex model to save computational time. In other words, a complete hysteresis cycle was not performed, but this does not undermine the validity of the results (43). The coordinates of the critical bifurcation points are extracted from these experiments and are listed in Table (1). There is no established method for determining the coordinates of bifurcation points when analysing the hysteresis of a complex model.

Only expertise and a deep understanding of the specific complex model can help identify the most likely values for these coordinates. For cGenie, the expertise of J. Gérard (co-author of this paper) was instrumental in identifying them. In the ATCM model, the critical points $\Psi^{\pm}$ for bifurcation must be the same, whether they are reached via temperature forcing or freshwater forcing. Moreover, we aim to find the best fit for temperature forcing, so we define $\Psi^{\pm} \equiv \Psi^{\pm}_{EXPA}$. Using these values, we compute the parameters $(a_1, b_1, c_1, d_1, e_{12})$, according to Eq. (7-10, 14), and the results are presented in Table (2). Based on the calibration of these parameters, the simplified hysteresis loop emulated by the ATCM is shown in Fig.(2). Since we calibrated the ATCM using the c_1 value from $EXPA$, the double-fold structure correctly passes exactly through the two bifurcation points identified on the cGenie hysteresis curve from the temperature forcing calibration experiment. However, this is not the case for $EXPB$, as will be explained in the Discussion section. Indeed, there is a 0.002 Sv difference between the F^{+}_{GIS} tipping point obtained from cGenie and the value computed by the ATCM, resulting in a relative difference between the two of 2.53%. Overall, the double-fold dynamics demonstrate a reasonably good calibration against the cGenie simulations.

	$\Psi^{+}\ [Adim]$	$\Psi^{-}\ [Adim]$	$T^{+}\ [°C]$	$T^{-}\ [°C]$	$F^{+}_{GIS}\ [Sv]$	$F^{-}_{GIS}\ [Sv]$
EXPA	0.545	0.022	5.93	3	/	/
EXPB	0.545	0.022	/	/	0.075	0.037

Table 1 : Critical bifurcation coordinates. The values are retrieved from the cGenie calibration sensitivity experiments $EXPA$ and $EXPB$ shown in Fig.(2).

a_1	b_1	c_1	d_1	e_{12}
0.851	-0.036	0.074	-0.024	-1.882

Table 2 : Internal dynamics parameter. The parameters are computed with the ATCM using Eq.(7-10,14)

The final parameter to calibrate in the ATCM to emulate cGenie is the parameter τ, which represents the characteristic timescale of the intrinsic dynamics of the AMOC. We apply the experimental protocol described in the Methods section, conducting a calibration experiment labelled $EXPC$ with cGenie. In this experiment, a step-by-step parameterized forcing of the freshwater flux is applied (see Fig.(3b)). The parameterization begins with a 0 Sv forcing for 2000 years, then increases the forcing by 0.05 Sv to slow down the AMOC intensity before returning to zero forcing. The same procedure is repeated after 6000 years, this time decreasing the freshwater flux by 0.05 Sv.

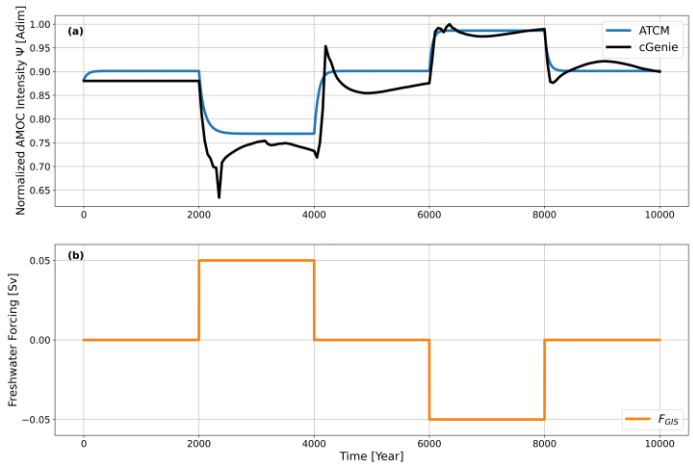

Figure 3: (a) Normalized AMOC intensity in the ATCM (blue) and cGenie (black) under varying freshwater flux forcing. **(b) Parameterization of freshwater flux** forcing in the calibration experiment $EXPC$.

By doing so, the AMOC is perturbed to observe the time it takes to transition between equilibrium states under an applied forcing. In Fig.(3a), the trajectory of the AMOC simulated by cGenie is shown in black, while the trajectory simulated by the ATCM is shown in blue. The goal is to calibrate the parameter τ to produce slopes in the ATCM trajectory that, for each transition between forcing levels, closely match the slopes computed by cGenie. After calibration, the best approximation of the ATCM to cGenie is achieved with a value of $\tau = 60\ \mathrm{yr}^{-1}$. The differences observed at the various plateaus between the AMOC and cGenie are due to the fact that the AMOC in cGenie has not yet fully stabilized to its equilibrium state. Additionally, the difference in the initial equilibrium state of the AMOC between cGenie and the ATCM arises from discrepancies in the preindustrial AMOC intensity values in cGenie and the ATCM (see Fig.(2)). These discrepancies will be discussed in the following section. Nevertheless, these differences do not compromise the calibration of the parameter τ because the focus is on reproducing the temporal evolution of the AMOC intensity during the transitions in forcing levels.

3.2 Validation of the emulator

To validate the emulator, we compare the ability of the ATCM to simulate the behaviour of the AMOC in cGenie using a new experiment, referred to as val_exp_1. This experiment represents a combination of forcing conditions distinct from those used in the calibration experiments. The val_exp_1 simulation spans 20,000 years and combines the thermal forcing from $EXPA$ – a linear increase in CO_2 concentration from 280 ppm to 2,800 ppm (see Fig. S1) – with a linear freshwater forcing increase from 0 Sv to 0.2 Sv (see Figs. S2 and S3).

Commented [AL7]: Retire the label '1' if Michel confirms that we only perform one validation experiment.

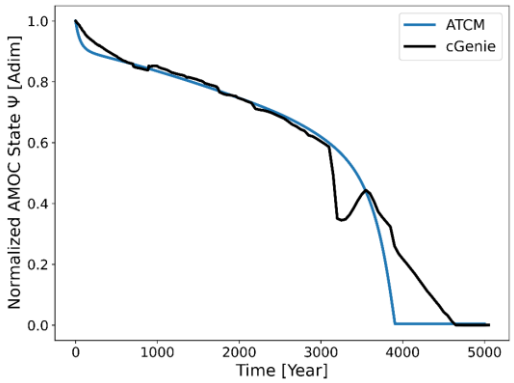

Figure 4 : Trajectories of the AMOC in the ATCM emulator (blue) and cGenie (black) in the val_exp_1 validation experiment.

The trajectories of the normalized AMOC intensity in both the emulator and the complex model are shown in Fig. (4). The ATCM, despite its simplified dynamics, captures the trajectory described by cGenie reasonably well, particularly during the first 3,000 years of the simulation. However, after 3,000 years, a sudden drop in AMOC intensity, followed by a partial recovery, is not captured by the ATCM. This discrepancy ultimately leads to a notable difference in the timing of the complete AMOC collapse. In the ATCM, the collapse occurs after 3,900 years, whereas in cGenie, it occurs after 4,650 years. As previously observed, the abrupt decrease in AMOC intensity in the ATCM during the early centuries of the simulation is due to differences in the equilibrium state associated with zero temperature forcing between the ATCM and cGenie, which result from the calibration process.

3.3 ATCM Integration within the SURFER Climate Model

To investigate the consequences of a complex model-consistent AMOC tipping element emulator under various climate scenarios, it is beneficial to integrate the ATCM emulator into a climate model. SURFER,

a reduced-complexity climate model with a process-based carbon cycle (39,40), is particularly well suited for this purpose. This model reliably simulates atmospheric CO_2 concentrations, global mean temperature changes, sea-level rise, and various ocean acidification metrics in response to anthropogenic greenhouse gas emissions, covering timescales from decades to millions of years. Version 3.0 of SURFER comprises 17 differential equations that describe carbon exchanges among six reservoirs: the atmosphere, terrestrial systems, upper, intermediate, and deep ocean layers, and deep-sea sediments (40). Additionally, it models temperature anomalies across ocean layers, ice sheet volumes for Greenland and Antarctica, and sea-level changes due to glacier dynamics. SURFER has proven effective for integrating tipping element dynamics into climate simulations, as demonstrated by Couplet et al. (32). Incorporating the ATCM emulator into a reduced-complexity climate model like SURFER provides a robust tool for examining a broad phase space and a wide range of realistic emission scenarios. This approach maintains realistic parameterizations while ensuring computational efficiency and manageable runtime. At the time of this project, version 3.0 of SURFER was not yet available. Therefore, we chose to integrate the ATCM into version 2.9 of SURFER (see Data Availability), a preliminary version of v3.0. There are no major differences between versions 2.9 and 3.0; notably, the changes pertain to the parameterization of SURFER carbon cycle, which is not a critical aspect for this study's objective of constructing an AMOC emulator coupled to a reduced-complexity climate model. To integrate the ATCM into SURFER v2.9, we decided to deactivate all components associated with tipping elements other than the AMOC and GIS, in order to avoid introducing errors into our analysis that would not stem from the AMOC and GIS.

Commented [AL8]: Should I explain that or not ? If yes is it ok ?

3.4 Results from the calibrated emulator : Critical Manifold and Sampling the Forcing Space

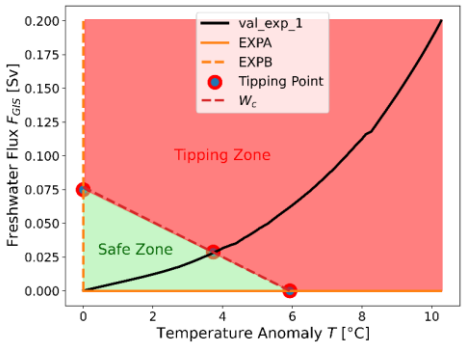

Figure 5 : Representation of the different forcings applied in the two calibration experiments *EXPA*, *EXPB* and the *val_exp*_1 validation experiment. The tipping points identified in the two calibration experiments are represented by the blue and red points. The red dashed line, W_c, defines the critical bifurcation manifold in the ATCM. The "Safe Zone" in the forcing space corresponds to the set of linear combinations of the two forcing variables that do not reach the bifurcation point. The "Tipping Zone" exceeds this bifurcation point.

Based on the calibration of the ATCM to cGenie, we can represent (see Fig.(5)) the two calibration experiments, $EXPA$ and $EXPB$, as well as the validation experiment val_exp_1, in the forcing variable space (T, F_{GIS}). This representation demonstrates the use of the emulator as a tool for mapping the forcing space of a given complex model. The critical manifold W_c is defined as follows,

$$W_c(T) = \frac{d_1}{e_{12}}(T^+ - T). \tag{15}$$

This manifold delineates the forcing space into two regions: one where the linear combinations of the variables T and F_{GIS} do not lead to a tipping of the AMOC in the emulator, and another where such combinations would eventually cause the AMOC to tip into an alternative equilibrium state. Despite the approximations inherent in the calibration process, the ATCM provides a valuable pre-diagnostic tool

for analysing forcing combinations that, if sustained for a sufficient duration (18), are expected to lead to a complete tipping of the AMOC.

As an application, we studied the response of the ATCM once integrated into SURFER under 15 different emission scenarios spanning SSP1-2.6 to SSP5-8.5 (see Fig.(S4)). Figure (6) illustrates the trajectories of these simulations in the forcing space (T, F_{GIS}). The critical manifold W_c is the same as in Fig. (5), obtained through the two calibration experiments, $EXPA$ and $EXPB$, conducted with cGenie. We observe that for 6 out of the 15 trajectories, the linear combination of the two forcing variables exceeds the critical bifurcation threshold of the AMOC. However, for two of these trajectories, the intensity and duration of this exceedance are sufficiently low to result in the overshoot-without-tipping phenomenon identified by Ritchie et al.(18). Finally, Figs.(5) and (6) highlight the importance of considering two forcing variables in the case of the AMOC. The inclusion of the freshwater flux as a second forcing variable significantly lowers the tipping point associated with temperature due to their combined effects.

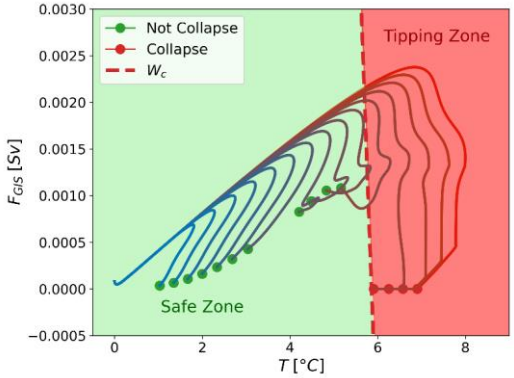

Figure 6: Representation of the fifteen emission scenarios spanning SSP1-2.6 to SSP5-8.5 (see Fig.(S4)) in the (T, F_{GIS}) forcing space. The dots indicate the state of the AMOC at the end of the 5000-year simulation. A green dot signifies $\Psi > \Psi^{+}$ corresponding to an active AMOC state, while a red dot indicates $\Psi < 0.1$, representing the collapsed state. The red dashed line, W_c, denotes the critical bifurcation manifold in the ATCM. The "Safe Zone" in the forcing space corresponds to the set of linear combinations of the two forcing variables that remain below the bifurcation threshold. Conversely, the "Tipping Zone" represents conditions that exceed this threshold.

---------- TO BE USED IF NEEDED----------

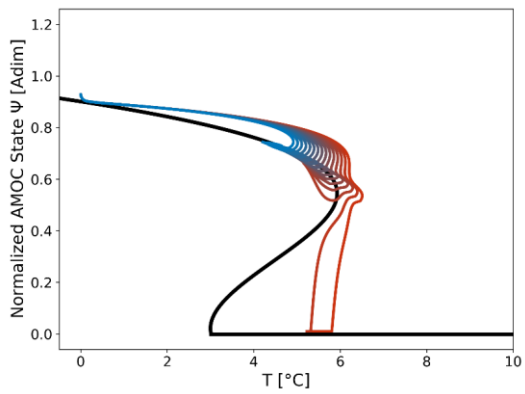

Figure 7 : Trajectories of the AMOC up to 5000 AD for 15 emission scenarios ranging from 3000 to 4000 PgC of total emissions since 1750. The black curve represents the bifurcation diagram of the ATCM. Six trajectories exceed the tipping point, but only two result in a collapse of the AMOC. An overshoot phenomenon without tipping occurs in four trajectories.

Commented [AL9]: Maybe I would like to use this kind of figure once I have confirmed the choice of parameterization of F_GIS. The idea is to shows scenarios with a tipping due to both effect of temperature and freshwater flux. The advantage would be to highlight the importance of having both variables forcing temperature and freshwater flux

4. Discussion

The challenge was to develop an AMOC emulator based on double-fold dynamics incorporating two forcing variables—temperature and freshwater flux— that could be effectively calibrated using complex models. To achieve this, we generalized the calibration method of Martinez Monteiro et al.(39) by assuming the feasibility of conducting independent forcing experiments for calibration.

The resulting AMOC Tipping Calibration Module (ATCM) has proven highly effective, as demonstrated in the Results section and Fig.(2). It successfully adjusts its simplified double-fold structure to closely replicate the cGenie complex model simulations. In the calibration based on cGenie experiments, the differences between the tipping points associated with F_{GIS} obtained from cGenie and those simulated by the ATCM are minimal. Specifically, this difference of $0.002\ Sv$, equivalent to a 2.5% error, falls within a reasonable uncertainty range reported in the literature (26, 28). To calibrate the characteristic timescale parameter τ, an effective experimental design with the complex model was demonstrated.

The differences between the ATCM and cGenie data can be attributed to two primary factors: the inherent limitations of the conceptual approach and constraints within the ATCM calibration module. The first is the inherent limitations of the simplified approach in fitting a double-fold structure to a complex hysteresis. These first limitations were known a priori. From a technical perspective, fitting a third-order polynomial to a complex curve is expected to result in a potentially significant discrepancy between the approximation and the reality described by the complex model. The challenge, therefore, lies in identifying the most effective method to minimize this inherent error as much as possible. Here, we explain the origins of these approximations and the measures taken to mitigate them.
Technically, the first source of error in the calibration module arises from the values of the independent term c_1, which must take the same value across all sensitivity experiments. As outlined in the Methods section, the coefficient is over-determined across the two sensitivity experiments. Consequently, a specific value of c_1 is selected based on one calibration experiment, but this value may not apply to the other. This approach implies that our simplified model is precisely calibrated to the bifurcation points of one calibration experiment (temperature forcing) but not the other (freshwater flux forcing). However, the decision to minimize error for temperature forcing is justified because this forcing is the dominant factor influencing the AMOC (13,14,44).
A second limitation of the ATCM calibration module is its inability to accurately align with the pre-industrial value of the AMOC. In their single-forcing parameter model, Martinez Montero et al. (39) were able to mathematically constrain the calibration model such that, under zero temperature anomaly forcing, the initial state of the simplified model corresponded precisely to the pre-industrial value of the tipping element. However, this approach cannot be generalized to models with two forcing parameters, as implementing such a constraint would introduce additional restrictions on the constant forcing values $F_{GIS}^{A}$and T_B, thereby limiting experimental flexibility.

Once the simplified dynamics of the AMOC were calibrated, the emulator was tested on one new experiment combining both forcing variables. The emulator successfully replicated the dynamics of cGenie up to the point where physical processes not accounted for by the ATCM induced significant changes in the AMOC's collapse dynamics in cGenie. These simplifications in the emulator's dynamics resulted in a notable discrepancy of 750 years in the precise timing of the AMOC's complete collapse. Thus, there is a cost in terms of the fidelity of the emulator's results, which may not be negligible.

However, we argue that the resulting emulator, which utilizes independent forcing experiments from complex models to calibrate tipping elements characterized by a double-fold bifurcation and two forcing variables, remains relevant. Indeed, the calibration produced provides a tool that is sufficiently close to the reality of the model being emulated to be usable. Finally, it is important to note that complex models, whether EMICs or even ESMs, still carry significant uncertainty regarding the exact location of the AMOC tipping points and, consequently, the timing of their collapse (5,28,44). In this context, the ATCM should not be regarded as a tool for delivering precise quantitative projections. While it is highly likely that the model values deviate from exact accuracy, we demonstrate that they are sufficiently well calibrated to remain plausible.

This is the key requirement for an AMOC tipping element emulator, enabling improved studies of the AMOC state under likely positions in its forcing space. As demonstrated in the Results section (see Fig. 6), the ATCM facilitates realistic sampling of the forcing space once integrated into a reduced-complexity climate model like SURFER. Where complex models face significant computational constraints, the presented emulator enables a large number of simulations to be performed at a much lower cost while maintaining consistency with more complex models. These easily obtained simulations also allow for the study of overshoot scenarios without AMOC tipping (18). Moreover, the unique critical variety W_c derived from each emulation defines the "identity card" of the complex model in the forcing space, reduced to its first-order dynamics. Comparing these critical varieties offers a method for assessing the inherent sensitivities of each model to AMOC collapse. Additionally, the calibration method presented here can be further generalized to include additional forcing variables (see Appendix). Another promising avenue is applying the ATCM methodology to the Greenland Ice Sheet (GIS) (see Appendix), creating a non-linear dynamics tool calibrated on complex models to explore possible cascading collapses between the AMOC and GIS (32, 34). Beyond the GIS, this approach to constructing tipping element emulators can be extended to other tipping elements, starting with the six additional elements whose initial parameterizations are included in SURFER v3.0 (40).

5. Conclusion

We have presented the AMOC Tipping Calibration Module (ATCM), an emulator of the AMOC tipping element dynamics based on a double-fold structure that, for the first time, incorporates two forcing variables that can be calibrated using experiments from complex models. To address this challenge, we adopted the methodological hypothesis that independent calibration experiments for each forcing variable could be conducted using the complex system. It was demonstrated that the constructed emulator satisfactorily reproduces the AMOC behaviour observed in the target complex model. Of course, the emulator is limited by its simplified dynamics, which result in noticeable differences between its outputs and those of the emulated complex model. Nevertheless, the ATCM's results fall within the uncertainty range reported in the literature for complex models, ensuring that its outputs remain plausible and coherent as an emulator. Furthermore, by accounting for both temperature anomalies and freshwater fluxes associated with Greenland Ice Sheet (GIS) melting, the emulator realistically incorporates this key dynamic in AMOC collapse. In addition, the ATCM allows for simulations of the AMOC with the significant computational advantages of an emulator, characterized by much shorter runtimes. Once integrated into a reduced-complexity climate model such as SURFER, the ATCM enables rapid yet realistic sampling of the forcing space under various emission scenarios. This capability allows for the efficient investigation of future AMOC dynamics using a reduced-complexity model that is finely calibrated to realistic emission scenarios.

Commented [AL10]: To update if I can add in the results section specific simulations showing this

Moreover, the calibration methodology described here can be readily applied to other tipping elements. A promising next step would be to calibrate a GIS emulator in a similar manner, providing a tool capable of modelling cascading collapses between the AMOC and GIS when calibrated on a complex model. Finally, beyond the tool itself, this study has developed and validated a calibration method for simplified two-forcing dynamics based on complex models such as Earth System Models of Intermediate Complexity (EMIC). This work offers a framework for bridging the gap between conceptual models and complex models, enhancing our understanding of future tipping element dynamics. By doing so, it underscores the urgent need for strong and immediate mitigation policies to address the risks posed by such critical system collapses.

Data and software availability

The code used in this study is publicly available on the following GitHub repository: https://github.com/VUB-HYDR. The *ATCM.ipynb* Jupyter Notebook contains the Python code where the ATCM is defined, calibrated, and validated using cGenie simulations. The *SURFER_v2.9_ATCM.ipynb* Jupyter Notebook contains the integration of the ATCM into the SURFER v2.9 climate model. These two notebooks were used to generate all the figures presented in this paper. The v2.9 version of SURFER, prior to the integration of the ATCM, is available in the *SURFER_v2.9.ipynb* notebook. The emission scenario data required to run the simulations implemented in SURFER can be found in the *data/SURFER/* directory within the GitHub repository. The data from the cGenie simulations (*EXPA*, *EXPB*, *EXPC* and *val_exp_1*) are accessible through the following Zenodo repository: https://zenodo.org/records/14514230.

Competing interests

No competing interests were disclosed.

Grant information

The majority of the technical work in this paper originates from the MSc Thesis of A. Laridon, completed in 2024 at UCLouvain (43) under the guidance of Prof. Crucifix. The writing and finalization of the research for this article were conducted at the beginning of A. Laridon's PhD thesis under the guidance of Prof. Thiery at VUB. The PhD is funded by the FWO under File Number: 1151225N.

Acknowledgements

This section should acknowledge anyone who contributed to the research or the article but who does not qualify as an author based on the criteria provided earlier (e.g. someone or an organization that provided writing assistance). Please state how they contributed; authors should obtain permission to acknowledge from all those mentioned in the Acknowledgements section.

Commented [AL11]: In my case I don't have this since all contributors are co-authors of the paper right ?

References

1. Stocker TF. Chapter 1 - The Ocean as a Component of the Climate System. In: Siedler G, Griffies SM, Gould J, Church JA, editors. International Geophysics [Internet]. Academic Press; 2013 [cited 2024 Dec 10]. p. 3–30. (Ocean Circulation and Climate; vol. 103). Available from: https://www.sciencedirect.com/science/article/pii/B9780123918512000015

2. Jackson LC, Kahana R, Graham T, Ringer MA, Woollings T, Mecking JV, et al. Global and European climate impacts of a slowdown of the AMOC in a high resolution GCM. Clim Dyn. 2015 Dec 1;45(11):3299–316.

3. Liu W, Fedorov AV, Xie SP, Hu S. Climate impacts of a weakened Atlantic Meridional Overturning Circulation in a warming climate. Sci Adv. 2020 Jun 26;6(26):eaaz4876.

4. Lenton T, Held H, Kriegler E, Hall JW, Lucht W, Rahmstorf S, et al. Tipping elements in the Earth's climate system. Proc Natl Acad Sci. 2008 Feb 12;105(6):1786–93.

5. Lenton T, Laybourn L, Armstrong McKay D, Loriani S, Abrams JF, Lade SJ, et al. Global Tipping Point Report 2023 [Internet]. UK: University of Exeter; 2023. Available from: https://report-2023.global-tipping-points.org/

6. Van Westen RM, Kliphuis M, Dijkstra HA. Physics-based early warning signal shows that AMOC is on tipping course. Sci Adv. 2024 Feb 9;10(6):eadk1189.

7. Zickfeld K, Eby M, Weaver AJ. Carbon-cycle feedbacks of changes in the Atlantic meridional overturning circulation under future atmospheric CO2. Glob Biogeochem Cycles [Internet]. 2008 [cited 2024 Apr 4];22(3). Available from: https://onlinelibrary.wiley.com/doi/abs/10.1029/2007GB003118

8. Brovkin V, Brook E, Williams JW, Bathiany S, Lenton TM, Barton M, et al. Past abrupt changes, tipping points and cascading impacts in the Earth system. Nat Geosci. 2021 Aug;14(8):550–8.

9. Rocha JC, Peterson G, Bodin Ö, Levin S. Cascading regime shifts within and across scales. Science. 2018 Dec 21;362(6421):1379–83.

10. Buckley MW, Marshall J. Observations, inferences, and mechanisms of the Atlantic Meridional Overturning Circulation: A review. Rev Geophys. 2016;54(1):5–63.

11. Goosse H. Climate System Dynamics and Modelling: [Internet]. 1st ed. Cambridge University Press; 2015 [cited 2024 Apr 20]. Available from: https://www.cambridge.org/highereducation/books/climate-system-dynamics-and-modelling/C8FC9D02159C8D9FD2146976AA8D28A6#contents

12. Stocker TF, Schmittner A. Influence of CO2 emission rates on the stability of the thermohaline circulation. Nature. 1997 Aug;388(6645):862–5.

13. Levang SJ, Schmitt RW. What Causes the AMOC to Weaken in CMIP5? J Clim. 2020 Feb 15;33(4):1535–45.

14. Gérard J, Crucifix M. Diagnosing the causes of AMOC slowdown in a coupled model: a cautionary tale. Earth Syst Dyn. 2024 Mar 22;15(2):293–306.

15. Bakker P, Schmittner A, Lenaerts JTM, Abe-Ouchi A, Bi D, van den Broeke MR, et al. Fate of the Atlantic Meridional Overturning Circulation: Strong decline under continued warming and Greenland melting. Geophys Res Lett. 2016;43(23):12,252-12,260.

16. Böning CW, Behrens E, Biastoch A, Getzlaff K, Bamber JL. Emerging impact of Greenland meltwater on deepwater formation in the North Atlantic Ocean. Nat Geosci. 2016 Jul;9(7):523–7.

17. Jackson LC, Alastrué de Asenjo E, Bellomo K, Danabasoglu G, Haak H, Hu A, et al. Understanding AMOC stability: the North Atlantic Hosing Model Intercomparison Project. Geosci Model Dev. 2023 Apr 6;16(7):1975–95.

18. Ritchie P, Karabacak Ö, Sieber J. Inverse-square law between time and amplitude for crossing tipping thresholds. Proc R Soc Math Phys Eng Sci. 2019 Feb 27;475(2222):20180504.

19. Stommel H. Thermohaline Convection with Two Stable Regimes of Flow. Tellus. 1961;13(2):224–30.

20. Wang S, Foster A, Lenz EA, Kessler JD, Stroeve JC, Anderson LO, et al. Mechanisms and Impacts of Earth System Tipping Elements. Rev Geophys. 2023;61(1):e2021RG000757.

21. Jackson LC, Wood RA. Hysteresis and Resilience of the AMOC in an Eddy-Permitting GCM. Geophys Res Lett. 2018;45(16):8547–56.

22. Rahmstorf S, Box JE, Feulner G, Mann ME, Robinson A, Rutherford S, et al. Exceptional twentieth-century slowdown in Atlantic Ocean overturning circulation. Nat Clim Change. 2015 May;5(5):475–80.

23. Caesar L, Rahmstorf S, Robinson A, Feulner G, Saba V. Observed fingerprint of a weakening Atlantic Ocean overturning circulation. Nature. 2018 Apr;556(7700):191–6.

24. Clement AC, Peterson LC. Mechanisms of abrupt climate change of the last glacial period. Rev Geophys [Internet]. 2008 [cited 2024 Dec 9];46(4). Available from: https://onlinelibrary.wiley.com/doi/abs/10.1029/2006RG000204

25. Rahmstorf S. Ocean circulation and climate during the past 120,000 years. Nature. 2002 Sep;419(6903):207–14.

26. Rahmstorf S, Crucifix M, Ganopolski A, Goosse H, Kamenkovich I, Knutti R, et al. Thermohaline circulation hysteresis: A model intercomparison. Geophys Res Lett [Internet]. 2005 [cited 2023 Oct 22];32(23). Available from: https://onlinelibrary.wiley.com/doi/abs/10.1029/2005GL023655

27. Weijer W, Cheng W, Drijfhout SS, Fedorov AV, Hu A, Jackson LC, et al. Stability of the Atlantic Meridional Overturning Circulation: A Review and Synthesis. J Geophys Res Oceans. 2019;124(8):5336–75.

28. Armstrong McKay DI, Staal A, Abrams JF, Winkelmann R, Sakschewski B, Loriani S, et al. Exceeding 1.5°C global warming could trigger multiple climate tipping points. Science. 2022 Sep 9;377(6611):eabn7950.

29. Ditlevsen P, Ditlevsen S. Warning of a forthcoming collapse of the Atlantic meridional overturning circulation. Nat Commun. 2023 Jul 25;14(1):4254.

30. Wood RA, Rodríguez JM, Smith RS, Jackson LC, Hawkins E. Observable, low-order dynamical controls on thresholds of the Atlantic meridional overturning circulation. Clim Dyn. 2019 Dec 1;53(11):6815–34.

31. Claussen M, Mysak L, Weaver A, Crucifix M, Fichefet T, Loutre MF, et al. Earth system models of intermediate complexity: closing the gap in the spectrum of climate system models. Clim Dyn. 2002 Mar 1;18(7):579–86.

32. Couplet V, Wunderling N, Crucifix M. Tipping interactions and cascades on multimillennial time

scales in a model of reduced complexity. 2024;

33. Dekker MM, von der Heydt AS, Dijkstra HA. Cascading transitions in the climate system. Earth Syst Dyn. 2018 Nov 6;9(4):1243–60.

34. Sinet S, von der Heydt AS, Dijkstra HA. AMOC Stabilization Under the Interaction With Tipping Polar Ice Sheets. Geophys Res Lett. 2023;50(2):e2022GL100305.

35. Wunderling N, Donges JF, Kurths J, Winkelmann R. Interacting tipping elements increase risk of climate domino effects under global warming. Earth Syst Dyn. 2021 Jun 3;12(2):601–19.

36. Liu W, Liu Z. A Diagnostic Indicator of the Stability of the Atlantic Meridional Overturning Circulation in CCSM3. J Clim. 2013 Mar 15;26(6):1926–38.

37. Rahmstorf S. On the freshwater forcing and transport of the Atlantic thermohaline circulation. Clim Dyn. 1996 Nov 1;12(12):799–811.

38. de Vries P, Weber SL. The Atlantic freshwater budget as a diagnostic for the existence of a stable shut down of the meridional overturning circulation. Geophys Res Lett [Internet]. 2005 [cited 2024 Dec 10];32(9). Available from: https://onlinelibrary.wiley.com/doi/abs/10.1029/2004GL021450

39. Martínez Montero M, Crucifix M, Couplet V, Brede N, Botta N. SURFER v2.0: a flexible and simple model linking anthropogenic CO_2 emissions and solar radiation modification to ocean acidification and sea level rise. Geosci Model Dev. 2022 Nov 9;15(21):8059–84.

40. Couplet V, Martínez Montero M, Crucifix M. SURFER v3.0: a fast model with ice sheet tipping points and carbon cycle feedbacks for short and long-term climate scenarios. EGUsphere. 2024 Sep 11;1–77.

41. Ridgwell A. cGENIE.muffin EMIC Documentation. 2022; Available from: https://www.seao2.info/mymuffin.html

42. Marsh R, Sóbester A, Hart EE, Oliver KIC, Edwards NR, Cox SJ. An optimally tuned ensemble of the 'eb_go_gs' configuration of GENIE: parameter sensitivity and bifurcations in the Atlantic overturning circulation. Geosci Model Dev. 2013 Oct 21;6(5):1729–44.

43. Laridon Amaury. Development of a Simplified Dynamics Emulator and Investigation of Cascading Collapses of the AMOC and Greenland Ice Sheet in a Climate Model [Internet]. UCLouvain; 2024. Available from: https://dial.uclouvain.be/memoire/ucl/object/thesis:46552

44. Liu W, Xie SP, Liu Z, Zhu J. Overlooked possibility of a collapsed Atlantic Meridional Overturning Circulation in warming climate. Sci Adv. 2017 Jan 6;3(1):e1601666.

Supplementary Materials :

Connecting Complex and Simplified Models of Tipping Elements: A Nonlinear Two-Forcing Emulator for the Atlantic Meridional Overturning Circulation

Amaury Laridon[1], Victor Couplet[2], Justin Gérard[2], Wim Thiery[1], Michel Crucifix[2]

[1]Vrije Universiteit Brussel, Department of Water and Climate, bclimate Research Group, Brussels, Belgium.
[2]UCLouvain, Earth and Life Institute, Louvain-La-Neuve, Belgium.
Corresponding author : Amaury.Laridon@vub.be

1. GIS Calibration

It is possible to apply the same calibration module, that relies on the independent forcing calibration experiments assumptions, on the GIS model Eq.(2),

$$\frac{dV}{dt} = \big(-V^3 + a_2V^2 + b_2V + c_2 + d_2T + e_{21}(1-\Psi)\big)\mu_V(V). \tag{a}$$

For the GIS, we must calibrate the coefficients a_2, b_2, c_2, d_2, and e_{21}. In this case, the same operational assumptions described for the application of the calibration module to the AMOC are applicable. Specifically, two calibration experiments are required: one providing the evolution of the GIS volume over time under forcing exclusively by the temperature anomaly while keeping the AMOC intensity fixed, and another under the opposite condition, where the GIS volume evolves with forcing exclusively by the AMOC intensity. In this context, the coordinates of the bifurcation points are determined by,

$$\{V^+, T_V^+, \Psi_V^+, V^-, T_V^-, \Psi_V^-\}. \tag{b}$$

We denote $EXPC$, in the case of the GIS as the first calibration experiment of the GIS volume in relation to temperature, in which the forcing from the AMOC intensity is held constant at an arbitrary value $\Psi_V = \Psi_V^C$. In this case, Eq.(2) is written as,

$$\frac{dV}{dt} = (-V^3 + a_2V^2 + b_2V + c_2 + e_{21}(1-\Psi^C) + d_2T)\mu_V(V). \tag{c}$$

This first sensitivity experiment provides us with the data for the following bifurcation points,

$$\{(V^+, T_V^+), (V^-, T_V^-)\}. \tag{d}$$

In this case with a single forcing variable, the method of Martinez-Monteiro et al.(39) yields,

$$a_2 = \frac{3(V^- + V^+)}{2}, \tag{e}$$

$$b_2 = -3V^-V^+, \tag{f}$$

$$c_2 + e_{21}(1-\Psi^C) = \frac{T_V^+V^{-^2}(V^- - 3V^+) - T_V^-V^{+^2}(V^+ - 3V^-)}{2(T_V^- - T_V^+)}, \tag{g}$$

$$d_2 = -\frac{(V^+ - V^-)^3}{2(T_V^+ - T_V^-)}. \tag{h}$$

Finally, we refer to $EXPD$ as the second sensitivity experiment in which we fix the global mean

temperature $T_V = T_V^D$ at an arbitrary value but vary the intensity of the AMOC Ψ_V. This sensitivity experiment provides us with the coordinates of the following bifurcation points,

$$\{(V^+, \Psi_V^+), (V^-, \Psi_V^-)\} \quad \text{(i)}$$

while equation Eq.(2) takes the following form:

$$\frac{dV}{dt} = \left(-V^3 + a_2 V^2 + b_2 V + c_2 + d_2 T^D + e_{21}(1 - \Psi)\right)\mu_V(V). \quad \text{(j)}$$

We cannot apply exactly the same calculation procedures for the coefficients due to the formulation of the AMOC forcing, which has a different form than those encountered before. We need to slightly adjust the calculation for the coefficients $c_2 + d_2 T^D, e_{21}$ although the methodology to find them remains the same as above. Therefore, we obtain:

$$c_2 + d_2 T^D = V^{+3} - a_2 V^{+2} - b_2 V^{\pm} e_{21}(1 - \Psi_V^+), \quad \text{(k)}$$

$$e_{21} = -\frac{(V^+ - V^-)^3}{2(\Psi_V^- - \Psi_V^+)}. \quad \text{(l)}$$

By combining the ATCM, which has demonstrated its validity, with this additional calibration section based on two complex model experiments of the GIS, we form the AMOC-GIS Tipping Cascade Calibration Module (AGTCCM). Further details can be found in the MSc Thesis by A. Laridon (43). This model uses the calibration technique based on the independent forcing hypothesis to better constrain the interactions between the AMOC and the GIS. This approach allows for the assessment, with the help of a conceptual yet calibrated model, of the joint evolution of the AMOC and GIS under realistic emission scenarios.

2. Parameterization of the AMOC with Three Forcing Variables

We present an example of a generalization of the ATCM in the case where a third forcing variable is added to the AMOC. Physically, it is interesting to separate the freshwater flux forcing into two components: F_{GIS}, associated with the melting of the GIS, and F_O, which is related to changes in the precipitation-evaporation $(P - E)$ balance over the Atlantic basin. Indeed, it has been shown that, due to climate warming, these variations could have a significant impact on the collapse of the AMOC (20–22). In this context, Laridon (43) developed the following parameterization, labelled $ParamB$, for the AMOC model.

$$\frac{d\Psi}{dt} = (-\Psi^3 + a_1 \Psi^2 + b_1 \Psi + c_1 + d_1 T + e_{12} F_{GIS}(V) + f F_O)\mu_\Psi(\Psi). \quad \text{(m)}$$

To apply the ATCM calibration module, an additional calibration experiment using a complex model is required. This experiment aims to perturb the AMOC by introducing a freshwater flux derived from the variability of the precipitation-evaporation $(P - E)$ balance, while maintaining constant freshwater flux from GIS melting and a fixed temperature anomaly. In this example with the AMOC, the operational framework becomes more challenging to implement; however, we can still easily derive the values of the calibration parameters, including the new parameter f. One observes the inherent limitation of generalizing to more forcing variables in this calibration method, namely that the independent parameter c_1 will now be determined by three factors rather than two. This introduces a new source of error, and the trade-off in the value at which c_1 should be calibrated will involve balancing three dynamics, rather than just two. Further details, as well as the calculated values of the coefficients, can be found in Laridon (43) and in the notebook *SURFER v2.9 ATCM.ipynb.*

3. cGenie Experiments

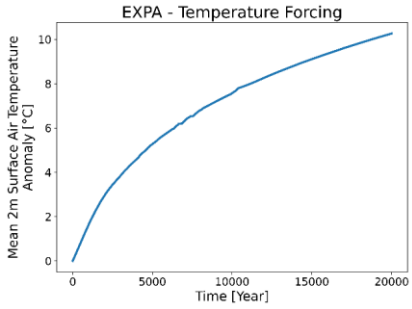

Supplementary Figure 1 | Temperature forcing in the calibration experiment *EXPA* and validation experiment *val_exp*_1 with cGenie. $EXPA$, consist of a 20,000-year simulation with a prescribed CO_2 forcing designed to generate a global atmospheric mean temperature anomaly. The forcing was parameterized as a linear function, increasing from 280 ppm to 2,800 ppm. Through the internal dynamics of cGenie, this forcing translated into a global mean 2-meter surface air temperature anomaly, starting from $T = 0°C$ and reaching $T = 10°C$ after 20,000 years.

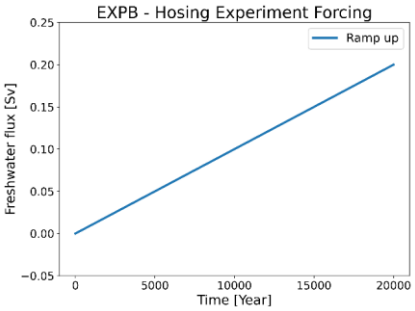

Supplementary Figure 2 | Hosing forcing in the calibration experiment *EXPB* and validation experiment *val_exp*_1 with cGenie. $EXPB$ involved a 20,000 year hosing simulation with freshwater flux forcing ranging from 0 Sv to 0.2 Sv, which is sufficient to induce the collapse of the AMOC in cGenie. The duration of $EXPB$ was choose to ensure that the AMOC is forced sufficiently slowly, allowing it to remain in equilibrium and produce an hysteresis experiment.

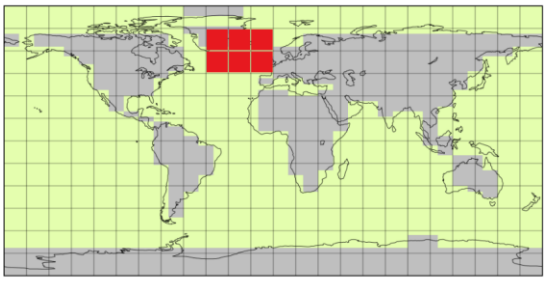

Supplementary Figure 3 | Hosing region in the calibration experiment EXPB and validation experiment *val_exp*_1 with cGenie. The freshwater hosing was applied between $50°N$ and $70°N$ and $45°W$ to $5°E$ to simulate the GIS melting.

4. Emission Scenarios

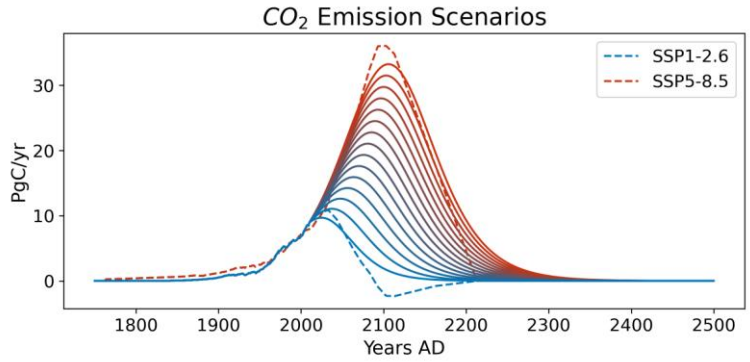

Supplementary Figure 4 | Fifteen emission scenarios spanning the SSP1-2.6 to SSP5-8.5 range used in SURFER. These scenarios account for cumulative emissions from 1000 to 5000 PgC into the atmosphere since 1750.